nature nanotechnology

SUPPLEMENTARY INFORMATION

DOI: 10.1038/NNANO.2009.192

# Supplementary Information

## for "Damping of Acoustic Vibrations in Gold Nanoparticles"

## I. Theoretical Model of Nanoparticle Dynamics in Fluid

In this section, we derive a theoretical model for the oscillatory motion of a bipyramidal nanoparticle immersed in fluid. The resonance frequency and damping rate of the oscillations are calculated by treating the nanoparticle as a bipyramidal rod immersed in a viscous fluid. The geometry considered is illustrated in Supplementary Figure 1.

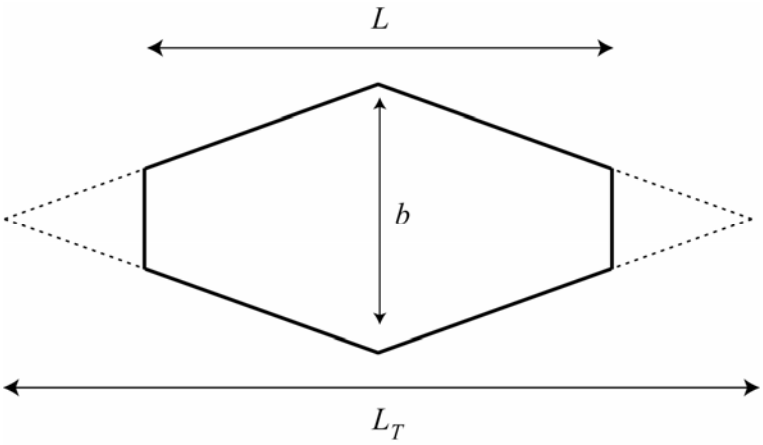


**Supplementary Figure 1:** Schematic of modelled nanoparticle showing dimensions. Dashed lines are projections of the sides. The $x$-direction is along the length of the rod, with the origin at the maximum width. The length of the rod is $L$, its "projected length" is $L_T$, and its maximum diameter is $b$.

We develop a self-consistent asymptotic theory in the limit $L >> b$, where the use of rod theory is rigorously justified. An analogous formalism has previously been used to describe the flexural vibrations of cantilever beams in fluid.[i,ii] The governing equation for the deformation, $U$, of the rod in the $x$-direction is[iii]

$$\frac{\partial}{\partial x}\left(EA\frac{\partial U}{\partial x}\right)-\rho_s A\frac{\partial^2 U}{\partial t^2}=-\int_{C_{side}}\boldsymbol{n}_s\cdot\boldsymbol{\sigma}_{fluid}\cdot\boldsymbol{i}\,dl \quad , \tag{S1}$$

where $A$ is the cross-sectional area of the rod, $\rho_s$ is the rod density, $\boldsymbol{\sigma}_{fluid}$ is the stress tensor in the fluid, $\boldsymbol{n}_s$ is the outward normal to the rod surface, $C_{side}$ is the circumference of the cross section, and $E$ is Young's modulus. Assuming an explicit time dependence of $\exp(-i\omega t)$, where $\omega$ is the angular frequency, we can immediately calculate the hydrodynamic force per unit length applied to the rod.

The viscous boundary layer over which vorticity diffuses is assumed to be thin in comparison to the nanoparticle width. In this limiting case, a local plane analysis can be performed, whereby the flow at the surface is given by Stokes' second problem for the oscillation of a flat plate in an unbounded fluid.[iv] For this classical solution, we readily obtain the hydrodynamic force per unit length:

$$F_{hydro} = \int_{C_{side}} \boldsymbol{n}_s \cdot \boldsymbol{\sigma}_{fluid} \cdot \boldsymbol{i}\, dl = C_{side}\, \mu\omega \sqrt{\frac{i\omega}{\nu}}\, u(x) \ , \tag{S2}$$

where $\nu = \mu/\rho$ is the kinematic viscosity, $\mu$ is the fluid shear viscosity, $\rho$ is the fluid density, and $u(x)$ is the spatial dependence of the displacement $U(x,t)$.

We assume that the width of the rod varies linearly with distance away from $x = 0$ and is symmetric about this plane; see Supplementary Figure 1. That is,

$$A(x) = A_0\left(1 - \frac{2x}{L_T}\right)^2 \ , \qquad C_{side} = C_0\left(1 - \frac{2x}{L_T}\right), \tag{S3}$$

where $A_0$ and $C_0$ are the cross sectional area and circumference at $x = 0$, respectively. Note that $L_T$ is the projected length of the rod (see Supplementary Figure 1), whereas $L$ is the actual length.

We then calculate the Rayleigh quotient for equation (S1):

$$\overline{\omega}^2 \equiv \left(\frac{L^2\rho_s}{E}\right)\omega^2 = \frac{\int_0^{\frac{1}{2}\frac{L}{L_T}} (1-2x)^2 \left(u'(x)\right)^2 dx}{\int_0^{\frac{1}{2}\frac{L}{L_T}} (1-2x)(1-2x+\Lambda)\left(u(x)\right)^2 dx} \ , \tag{S4}$$

where

$$\Lambda = \alpha \frac{\rho}{\rho_s} \frac{1+i}{\sqrt{\beta_0}} , \qquad \beta_0 = \frac{2C_0^2 \omega}{\nu} , \qquad \alpha = \frac{C_0^2}{A_0} , \tag{S5}$$

and the *x*-coordinate in equation (S4) and below is scaled with respect to $L_T$.

Next, the mode shape of the deformation is required. We approximate this by the mode shape of the rod in the absence of the fluid. Using equation (S1), the mode shapes are given by

$$u(x) = \frac{\sin(\Omega x)}{1-2x} , \tag{S6}$$

where $\Omega$ is specified by the following eigenvalue equation:

$$\Omega\left(1-\frac{L}{L_T}\right)\cos\left(\frac{\Omega L}{2L_T}\right)+2\sin\left(\frac{\Omega L}{2L_T}\right)=0 . \tag{S7}$$

We perform an asymptotic analysis of the solution to this eigenvalue equation, from which we obtain, for the lowest-order mode,

$$\Omega = 2\pi + \frac{2}{3}(2\pi)^3\left(1-\frac{L}{L_T}\right)^3 + O\left(\left[1-\frac{L}{L_T}\right]^4\right) . \tag{S8}$$

Equation (S8) establishes that the vacuum frequencies are weakly dependent on the ratio $L/L_T$ and are given by

$$\omega_{vac} = \frac{\Omega}{L_T}\sqrt{\frac{E}{\rho_s}} \approx \frac{2\pi}{L_T}\sqrt{\frac{E}{\rho_s}} . \tag{S9}$$

Substituting the mode shape in equation (S6) into the Rayleigh quotient, equation (S4), gives

DOI: 10.1038/NNANO

$$\overline{\omega}^2 \equiv \left(\frac{L_T^2 \rho_s}{E}\right)\omega^2 \cong \frac{4\pi^2}{1+\left(2.44-9.87\left[1-L/L_T\right]^2\right)\Lambda} + O\left(\left[1-L/L_T\right]^3\right) . \qquad \text{(S10)}$$

Equation (S10) enables the fundamental angular resonance frequency $\omega_R$ and quality factor $Q_{fluid}$ of the rod in fluid to be calculated. For a circular cross section, $\alpha = 4\pi$, and we obtain

$$\omega_R = \omega_{vac}\left\{1+\Gamma\left(\omega_R\right)\right\}^{-1/2} , \qquad Q_{fluid} = 1+\frac{1}{\Gamma\left(\omega_R\right)}, \qquad \text{(S11)}$$

where

$$\Gamma(\omega) = 2.44\left(1-4.05\left[1-L/L_T\right]^2\right)\frac{\rho}{\rho_s}\frac{1}{\sqrt{\beta}} , \qquad \beta = \frac{\omega R^2}{2\nu} , \qquad \text{(S12)}$$

and $R$ is the maximum radius of the rod.

The model of a damped harmonic oscillator is used to extract the resonance frequency and quality factor from measurements (see equation (1)). This implicitly assumes that the hydrodynamic load is independent of frequency, an assumption that is valid only if $Q_{fluid} >> 1$ (see Reference i). This means that the above theory is applicable only in the same limit of high quality factor, which is consistent with the assumption of thin viscous boundary layers. In this limit, equations (S11) and (S12) predict that the damping rate is proportional to $\sqrt{\mu\rho}$; this scaling behaviour is observed experimentally, as described in Section II. We note that this limit is not valid for particles in glycerol, so the theory can be used only to describe particles in the three other solvents investigated.

For quantitative comparison to experiment, we use literature values for the properties of the solvents and of gold[v] and particle dimensions measured from transmission-electron-microscope images ($L$ = 78.7 nm, $b$ = 28.4 nm, and $L_T$ = 105 nm). No adjustable parameters are used. Results of the calculations are reported in Supplementary Table 1, where they are compared to measurement results.

| Solvent | Viscosity $\mu$ (cP) | Density $\rho$ (g/cm$^3$) | Homogeneous Damping Time $T_1$ (ps) | Experimental Resonant Frequency $f$ (GHz) | Experimental $Q_1$ |
|---|---|---|---|---|---|
| Methanol | 0.54 ± 0.02 | 0.791 | 286 ± 40 | 19.2 ± 0.1 | 17.3 ± 2.4 |
| Water | 0.89 ± 0.07 | 0.998 | 261 ± 10 | 19.1 ± 0.3 | 15.7 ± 0.6 |
| Ethylene Glycol | 16.1 ± 0.8 | 1.11 | 137 ± 12 | 20.0 ± 0.6 | 8.6 ± 0.8 |
| Glycerol | 934 ± 63 | 1.26 | 28 ± 10 | 18 ± 2 | 1.6 ± 0.6 |

| Solvent | Viscosity $\mu$ (cP) | Density $\rho$ (g/cm$^3$) | Theoretical $Q_{fluid}$ | Theoretical Resonant Frequency (GHz) | Theoretical $Q_1$ | Viscous Boundary Layer Thickness (nm) |
|---|---|---|---|---|---|---|
| Methanol | 0.54 ± 0.02 | 0.791 | 58.6 ± 2.2 | 19.8 | 17.5 ± 1.5 | 3.3 |
| Water | 0.89 ± 0.07 | 0.998 | 41 ± 3 | 19.8 | 15.5 ± 1.2 | 3.8 |
| Ethylene Glycol | 16.1 ± 0.8 | 1.11 | 9.9 ± 0.5 | 18.9 | 7.1 ± 0.2 | 15 |
| Glycerol | 934 ± 63 | 1.26 | (2.1 ± 0.1) | (13.8) | (1.9 ± 0.1) | 108 |

**Supplementary Table 1.** Measured and calculated results for acoustic vibrations in a sample of bipyramidal gold nanoparticles, capped with PSS, for different solvents. Reported viscosities and densities are literature values. Error estimates for the viscosities correspond to variation over a temperature range of ± 2 °C and are the source of error estimates for theoretically calculated quality factors, $Q_{fluid}$, due to viscous damping; the temperature dependence of density is much smaller. Theoretical values of total homogeneous quality factors, $Q_1$, are determined using an intrinsic quality factor $Q_{intrinsic}$ = 25 ± 3. Theoretical results for glycerol are shown in parentheses because the model is not applicable for this system.

DOI: 10.1038/NNANO

## II. Scaling Relations for Fluid Damping

In order to experimentally demonstrate the dominant physical processes responsible for fluid damping, we perform a scaling analysis of the homogeneous damping rates against different fluid properties. This analysis provides experimental verification of the rigorous theory derived in Section I.

We consider three possibilities: (a) damping rates that scale with the fluid's acoustic impedance, equal to $\sqrt{\kappa\rho}$, where $\kappa$ is the bulk modulus of the fluid and $\rho$ is the fluid density, which is expected when fluid compressibility dominates and energy is carried away by sound waves;[vi,vii] (b) damping rates that scale with the fluid viscosity, $\mu$, which is expected when the particle vibrations generate thick viscous boundary layers;[i,ii,viii] and (c) damping rates that scale with $\sqrt{\mu\rho}$, which is expected when viscous boundary layers are thin (see Section I). Supplementary Figure 2 shows the measured homogeneous damping rates plotted against these variables; literature values are used for the fluid properties.[v] It can clearly be seen that only the last scaling provides a good description of the experimental data.

This observation is consistent with the physical situation for high-frequency vibration of metal nanoparticles in methanol, water, and ethylene glycol. As shown in Supplementary Table 1, viscous boundary layers in these fluids are small compared to the particle widths. In addition, compressibility of the fluid would be important only if the acoustic wavelength in the fluid were comparable to or smaller than the dominant hydrodynamic length scale of the flow generated by the vibrating particle.[iv] The gold nanoparticles oscillate at 20 GHz, and the speed of sound in the fluid ranges from 1100 – 1900 m/s, giving acoustic wavelengths in the range 55 – 95 nm. This greatly exceeds the dominant length scale for the flow, which is dictated by the minimum of the rod width and the viscous penetration depth. Furthermore, we note that longitudinal oscillations of the nanoparticles, in the limit where the particle diameter is small compared to the length, are independent of fluid compressibility, since they generate unidirectional flow that is pressure invariant. This salient feature is implicit in the theoretical model presented in Section I.

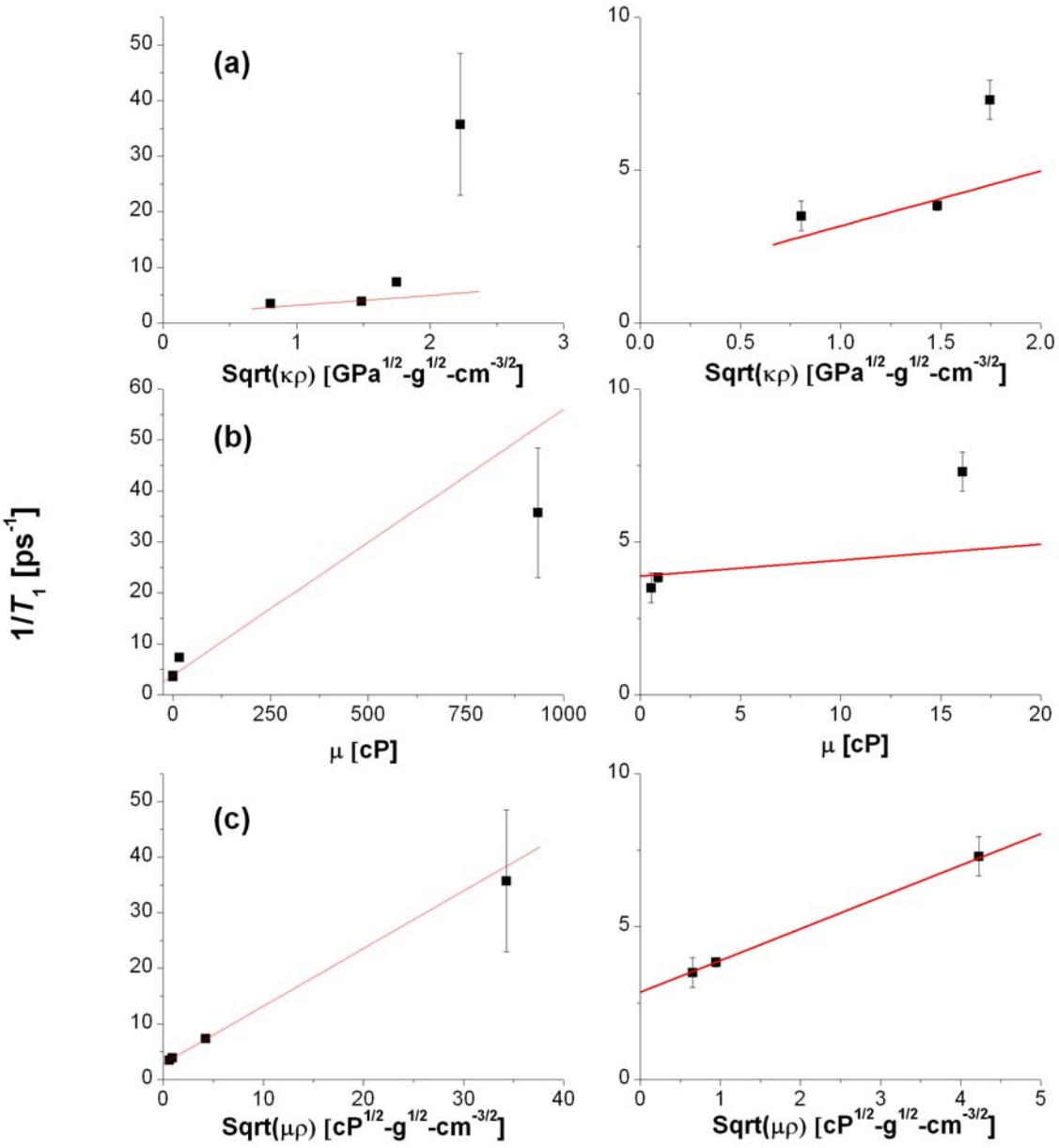


**Supplementary Figure 2:** Scaling relations for homogeneous damping rates. The homogeneous damping rates, $1/T_1$, in four different solvents are plotted against different mechanical properties of the fluid, from top to bottom: (a) acoustic impedance, equal to the square root of bulk modulus, $\kappa$, times density, $\rho$, (b) viscosity, $\mu$, and (c) square root of viscosity times density. Right-hand panels show the same data as the left-hand panels, but on different scales.

DOI: 10.1038/NNANO

## III. Fitting Transient Spectra

Approximating the linear extinction of the nanoparticle solution near the longitudinal plasmon resonance as a Lorentzian, the transient spectrum is expected to take on the following form:[ix]

$$\Delta A \propto \frac{1}{\Delta\omega^2 + \frac{1}{4}} - \frac{\gamma(t)}{\left[\Delta\Omega(t) - \Delta\omega\right]^2 + \frac{1}{4}\left[\gamma(t)\right]^2} \quad . \tag{S13}$$

This expression involves the following normalized frequencies: $\Delta\omega \equiv \omega - \Omega_o/\Gamma_o$, $\Delta\Omega(t) \equiv \Omega(t) - \Omega_o/Z_o$, and $\gamma(t) \equiv Z(t)/Z_o$, where $\omega$ is the probe frequency; $\Omega_o$ and $Z_o$ are the plasmon resonance frequency and linewidth, respectively, in the absence of the pump pulse; and $\Omega(t)$ and $Z(t)$ are the resonance frequency and linewidth for a pump-probe delay $t$. The values of $\Omega_o$ and $Z_o$ were determined by fitting the linear extinction spectrum to a Lorentzian over the range of the longitudinal plasmon resonance; these values were measured separately for each solvent and capping molecule used. The fitted values were then used to normalize the measured transient spectra, which were subsequently fit to equation (S13), yielding experimental values for the peak shift, $\Omega(t)$. The proportionality constant in equation (S13) depends on experimental parameters, including the pump spot size and the overlap volume between the pump and probe pulses, that are not known with great accuracy; however, the effect of changing the constant is simply to scale the fitted values of $\Omega(t)$ by a fixed value. Since we are interested only in the time dependence of this quantity, we report the fitting results in arbitrary units. In addition, the approximation of the ensemble spectrum by a Lorentzian ignores inhomogeneous broadening of the longitudinal plasmon resonance. Since this broadening is only about 25% of the homogeneous linewidth,[x] the approximation is expected to introduce a relatively small error and should have a negligible effect on the time dependence of $\Omega(t)$.

## IV. Finite-Element Simulations

Finite-element calculations were performed using the COMSOL software package (version 3.2). The particles were modeled as homogeneous, isotropic, elastic objects, whose mechanical parameters (Young's modulus, Poisson's ratio, and density) were assumed to be the same as those for bulk gold at room temperature.[xi] The shape of the particles in the model reflects the five-fold symmetry and rounded tips of realistic nanoparticles. Since only symmetric vibrational modes can be excited by the pump laser, we considered only the lowest-frequency symmetric eigenmode, which is analogous to the fundamental extensional mode of a cylinder. No mechanical losses were included in these simulations, which serve to determine vibrational frequencies only.

## V. Contribution of Capping Molecules to Intrinsic Damping

Intrinsic damping of acoustic vibrations can have contributions due to mechanisms occurring in the gold cores of the nanoparticles and due to the surface layer of organic molecules. To obtain an initial estimate of the relative importance of surface and bulk effects, we made measurements on a second sample with a series of different capping molecules. The inhomogeneity of this sample was somewhat larger than that of the first sample, making it difficult to fit the measurements in the same way. Instead, we approximated the decay of the vibrations as a single exponential with a time constant $\tau_{decay}$ given by $1/\tau_{decay} = 1/T_1 + 1/T_2^*$, where $T_1$ and $T_2^*$ are the homogeneous and inhomogeneous damping times, respectively. Although this can provide only an approximation of the true damping, it is adequate for a first estimate of the importance of the capping molecules.

As shown in Supplementary Table 2, the damping times are relatively insensitive to changes in the capping molecules, considering the significant differences in the mechanical properties of the molecules. The cetyltrimethylammonium bromide (CTAB) double layer, for example, is soft and forms a weakly-bound micellar double layer around the particles; the poly-styrene sulfonic acid (PSS) layer coats the particle physically and is expected to have moderate stiffness in solution; and the alkanethiols are short, rigid molecules that are covalently bound to the gold surfaces.

| Capping Layer | Total Decay Time $\tau_{decay}$ (ps) |
|---|---|
| CTAB | 121 ± 3 |
| PSS | 106 ± 3 |
| Hexanethiol | 116 ± 3 |
| Dodecanethiol | 104 ± 4 |

**Supplementary Table 2.** Experimentally measured decay times of acoustic vibrations for a second sample of bipyramidal gold nanoparticles, in water, for different capping molecules.

We determined the inhomogeneous damping time $T_2^*$ for this sample, as for the first one, by simulating the oscillation period for a number of nanoparticles whose dimensions were measured from TEM images. Using this calculated value to determine homogeneous damping times, we estimate that the capping molecules cause a variation of up to 110 ps in the homogeneous damping time, corresponding to 26% of the intrinsic damping time.

## References

[i] Sader, J.E. Frequency response of cantilever beams immersed in viscous fluids with applications to the atomic force microscope. *J. Appl. Phys.* **84**, 64-76 (1998).

[ii] Van Eysden, C. A., & Sader, J. E. Frequency response of cantilever beams immersed in viscous fluids with applications to the atomic force microscope: Arbitrary mode order. *J. Appl. Phys.* **101**, 044908 (2007).

[iii] Love, A. E. H. *A Treatise on the Mathematical Theory of Elasticity* (Dover Publications, New York, 1944).

[iv] Batchelor, G. K. *An Introduction to Fluid Dynamics* (Cambridge University Press, 1967).

[v] Lide, D.R., Ed. *CRC Handbook of Chemistry and Physics, 89th Ed.* (CRC Press, Boca Raton, Florida, 2008).

[vi] Voisin, C., Chistofilos, D., Del Fatti, N. & Vallée, F. Environment effect on the acoustic vibration of metal nanoparticles. *Physica B* **316-317**, 89-94 (2002).

[vii] Saviot, L., Netting, C., & Murray, D. Damping by bulk and shear viscosity of confined acoustic phonons for nanostructures in aqueous solution. *J. Phys. Chem. B* **111**, 7457-7461 (2007).

[viii] Yum, K., Wang, Z., Suryavanshi, A., & Yu, M.-F. Experimental measurement and model analysis of damping effect in nanoscale mechanical beam resonators in air. *J. Appl. Phys.* **96**, 3933-3938 (2004).

[ix] Zadoyan, R. *et al*. Diagnostics of spectrally resolved transient absorption: Surface plasmon resonance of metal nanoparticles. *J. Phys. Chem. C* **111**, 10836-10840 (2007).

[x] Liu, M.Z. & Guyot-Sionnest, P. Mechanism of silver(I)-assisted growth of gold nanorods and bipyramids. *J. Phys. Chem. B* **109**, 22192-22200 (2005).

[xi] Materials Properties Database (MPDB), JAHM software, http://www.jahm.com